Advances in Nonlinear Variational Inequalities
ISSN: 1092-910X
Vol 27 No. 3 (2024)

MHNFSP: Design of an Efficient Model for Advanced MRI Image Classification Using Hybrid Neural Networks and Optimized Feature Selection Process

Swati k. Mohod [1], Rajesh D. Thakare[2]

[1]Reserach Scholar, Department of EE, Yeshwantrao Chavan College of Engineering, Nagpur

[2] Department of EE, Yeshwantrao Chavan College of Engineering, Nagpur

swatimohod6882@gmail.com, rdt2909@gmail.com

Article History:

Received: *16-02-2024*

Revised: *26-04-2024*

Accepted: *18-05-2024*

Abstract

In the field of medical imaging, particularly regarding magnetic resonance imaging (MRI) and the analysis of feature extraction in the MRI, there exists an immediate and pressing need for precision and clarity in the accuracy of such. Current methods, though useful, have inherent weaknesses with respect to dealing with noise, specific feature identification, and an ability to effectively merge different types of data. The explained developments show the need of innovation in MRI image classification, especially for distinguishing slight but critical variations in brain images and samples. These gaps underline the urgency for innovation in MRI image classification, especially for differentiating delicate nuances of brain images and samples. The proposed model has addressed these gaps through an innovative workflow for MRI image classification, identified by a novel, synergistic approach process. The workflow begins with the scrupulous acquisition of MRI and fMRI images, capturing the intricate structural and functional nuances of the brain. Image segmentation is employed for innovative execution using Fuzzy C-Means (FCM), picked for its excellent noise resistance and the advantage of soft clustering that is important for a more exact definition of the boundaries of the regions of interest in the image set. The feature extraction phase involves three phases with Fourier, Entropy, and Convolution features from an elevated perspective. This trio is very carefully picked to encapsulate a comprehensive image representation, harmonizing the shape, texture, and local structure. The workflow of this model is streamlined from the feature set with the employment of Whale Optimization, which quite efficaciously sieves the feature set, retaining the most informative while curtailing redundancy and overfitting issues within the process. Eventually, a Hybrid Convolutional Neural Network (CNN) emerges at the top of this model, incorporating Naive Bayes, k-Nearest Neighbors (kNN), Support Vector Machine (SVM), Logistic Regression (LR), and Multi-Layer Perceptron (MLP) methods. This selective multi-classifier classification provides a robust and heterogeneous set of functions for the classification. Tested on different OASIS and ADNI datasets and samples, this model has outperformed current methods with a 4.9% increase in precision, a 4.5% enhancement in accuracy, a 3.5% rise in recall, a 4.3% augmentation in AUC (Area Under the Curve), a 3.4% improvement in specificity, and a 2.9% cutdown in delay. Such advancements not only signify a great leap in MRI image classification but also carry very much significance for medical diagnosis and research, and that could see its way into the clinical field. In this model, the amalgamation of disparate methods sets a new benchmark in medical imaging, opening doors to better accuracy, higher efficiency, and greater reliability of diagnostic tools.

Keywords: Biomass Briquettes, Rice Husk Fuel, Energy Efficiency,

1. Introduction

Within the dynamics of medical imaging, analysis of Magnetic Resonance Imaging (MRI) acts as an indispensable step in the diagnosis and understanding of neurological disorders. The formulations of MRI, however, still grapple with classical methodologies with technical faults, such as sensitivity to noise and incomplete feature extraction capabilities. These hindrances have spurred the development of sophisticated models, emulating for MRI data processing as far as accuracy and precision are concerned. In this regard, the revolution of advance machine learning techniques opens up new avenues in the interpretation of medical images. As such, MRI image classification constitutes a foundation for early and precise diagnosis of brain disorders. In fact, the conventional approaches, mostly based on straightforward algorithms, have remained ineffective in harnessing the extent of the complex data presented in MRI scans. Thus, a model that comprehensively grasps the depth of MRI data and adapts to its varying characteristics is very required.

In light of this need, this paper proposes a model for MRI classification using a hybrid CNN. Essentially, the model is based on the integration of multiple classifiers, to take advantage of each one's strengths. This integration represents a significant departure from the conventional methods, putting forward an enhanced and comprehensive analytical tool. In this model, classifiers like Naive Bayes, k-Nearest Neighbors (kNN), Support Vector Machine (SVM), Logistic Regression (LR), and Multi-Layer Perceptron (MLP) are included. Each of the classifiers provides a unique dimension to the model, hence aiding in its competence to interpret MRI data effectively. The model begins with the careful collection of MRI and fMRI images. These are the foundation of the classification process, and they provide detailed insights into the brain's structural and functional features. Fuzzy C-Means (FCM) was selected because it aptly does image segmentation, most of the time in dealing with the challenging nuisance that accompanies MRI images. The outcomes of FCM form a soft clustering result, which is vital in accurately segmenting regions of interest in the brain scans.

Feature extraction within the model is a tripartite operation that includes Fourier, Entropy, and Convolution. This combination is expressly selected to capture a wide range of information about the images. The Fourier descriptors are useful in describing the contours of the segmented regions, the Entropy features highlight areas with distinct textural properties, and the Convolution features capture local patterns and structures in the images. This multiple feature set assures thorough representation of MRI data, hence necessary to ensure good classifications.

To optimize the model's performance, Whale Optimization is deployed in the feature selection step. This step is important as a dimensionality reduction step commonly taken in MRI image analysis, due to overfitting, among other possible risks. Whale Optimization offers an efficient search method, so it chooses the bestinformed features, giving less chance of overfitting while still ensuring streamlined results.

The introduction of this model into the field of medical imaging analysis means invariably that there is a new era of medical diagnosis. With the model based on this unique combination of advanced

feature extraction techniques, optimized feature selection, and a hybrid classification approach, it will find a very effective tool in MRI image analysis. The model has been tested on various datasets that show its effective nature, proving that it can, possibly, change the future of medical diagnosis, mainly in early diagnosis of and knowledge of neurological disorders. In this paper, the model is demonstrated in its complexity, methodology, the idea behind it, and the remarkable benefits that it carries to medical imaging processes.

Motivation & Contributions

The Motivation and Contribution section of a scientific paper delves into the underlying reasons that spurred the research, and the novel contributions it brings to the field. For MRI image classification, the motivation is the need to develop an advanced computational methodology to surpass shortcomings faced by current methods and recognize subtle alterations in brain structures using powerful machine learning techniques for improved diagnosis and understanding of neurological conditions.

Motivation:

In a moment of imperative change within the field of medical imaging, particularly MRI analysis, current methods, while having made appreciable strides, are still, in fact, holding back in face of noise interference, insufficient feature extraction, and wanting in the comprehensiveness of data interpretation. Such a gap in technology is even more noticeable in diagnosing subtle brain disorders that call for more sophisticated approaches. New avenues present in the rapidly evolving domains of machine learning and neural networks also give a new horizon in medical imaging. The motivation for this research lies in bridging the gap by developing a model that not only goes beyond the weaknesses in the current models but also in utilizing the novel approaches emerging in computational technology.

Contribution:

The main contribution of this work is the formation of a new hybrid MRI image classification model with the combination of a very advanced feature selection method and CNNs. This work's breakdown with such reasons:

- Hybrid Convolutional Neural Network (CNN): The model makes use of different classifiers—Naive Bayes, kNN, SVM, LR, and MLP—in combination, thus bringing a multi-dimensional perspective to the analysis of MRI. Such an approach is very rare; it allows the highlighting of the strengths of each classifier incorporated into the process of classification and, therefore, can bring greater accuracy and robustness in the classification process.

- Advanced Feature Extraction and Selection: The model uses the fusion of Fourier, Entropy, and Convolution features to provide a comprehensive representation of the MRI data samples. Feature selection has been further advanced through Whale Optimization to ensure that only relevant features are considered, hence cutting down the computational complexity and increasing efficiency of the model.

- Handling Noise and Complexity of Data: The model uses Fuzzy C-Means (FCM) specifically for image segmentation due to its efficiency in dealing with noise and providing soft clustering. The practical relevance is of utmost importance since MRI images require clarity and precision.

- Empirical Validation: The validation of the model was rigorously executed on both the OASIS and ADNI datasets, where it comes out on top of the current methods. Such empirical evidence not only validates the model but also carries its practical relevance to real-life applications.

- Implications for Medical Diagnosis and Research: The model's ability to classify MRI images with high accuracy has far-reaching implications for medical diagnosis, especially in detecting early brain disorders. It paves the way for more precise and early interventions that might influence outcomes for patients.

In a nutshell, the research sets a benchmark for improving the performance of medical image analysis. The model achieves a new level of accuracy and efficiency, where the use of advanced computational techniques for nuanced basis related to the MRI data is incorporated. This might provide inspiration for further medical research and diagnosis.

2. Review of existing models used for classification of MRI Image Sets

A recent trend in the increasing field of medical imaging, especially in the development of using MRI in Alzheimer's disease diagnosis, has brought about great developments in the recent past. This review outlines some of the studies that have contributed to this domain, bringing out the innovative approaches and methodologies that researchers have used to improve the accuracy and efficiency of AD diagnosis. Guan et al. [1] reported the use of an attention-guided autoencoder model to predict subjective cognitive decline progression using structural MRI. The method underscored the importance of focusing on specific regions of interest in the brain for early AD detection. Similarly, Dong et al. [2] investigated the association between hippocampal morphometry and plasma neurofilament light chain, offering insights into the nature of the biomarkers associated with cognitive impairment. The deep learning technique has become a particular center of interest during this period for analysis based on MRIProcess.Rashid et al. [3] presented Biceph-Net, a robust framework for Alzheimer's disease diagnosis using 2D-MRI scans and deep similarity learning. This approach highlighted the effectiveness of deep learning in capturing intricate patterns in MRI data samples. In a similar vein, Shamrat et al. [4] developed AlzheimerNet, a proposition for classifying Alzheimer’s disease stages based on functional brain changes in MRI images, emphasizing the potential of deep learning models in understanding disease progression.

Liu et al. [5] explored the risk prediction of Alzheimer's disease conversion in the mildly cognitively impaired population based on brain age estimation, showcasing the predictive power of MRI data samples.Chabib et al. [6] proposed DeepCurvMRI, a deep convolutional curvelet transform-based MRI approach for the early detection of Alzheimer’s disease, which illustrated the benefits of combining traditional image processing techniques with deep learning.

Jamalullah et al. [7] leveraged enhanced Manta Ray Foraging Optimization-based deep learning for biomedical Alzheimer’s disease diagnosis using brain MRI, highlighting the importance of optimization algorithms in deep learning frameworks. Rao and Aparna [8] provided a comprehensive

review on Alzheimer’s disease analysis through MRI images using deep learning techniques, summarizing the state-of-the-art methods and their effectiveness.

Pusparani et al. [9] introduced a novel approach for the diagnosis of Alzheimer’s disease using a convolutional neural network with select slices by landmark on the hippocampus in MRI images. This study demonstrated the significance of focusing on specific brain regions for more accurate diagnosis. Zhang et al. [10] explored explainable tensor multi-task ensemble learning based on brain structure variation for dynamic prediction of Alzheimer’s disease, emphasizing the need for interpretable and multi-faceted models in medical imaging scenarios.

Furthermore, Kim and Lee [11] focused on the classification of Alzheimer’s disease using an ensemble convolutional neural network with the LFA algorithm, reinforcing the trend towards ensemble methods for improved performance in AD diagnosis. Illakiya and Karthik [12] presented a dimension-centric proximate attention network and Swin Transformer for age-based classification of mild cognitive impairment from brain MRI, showcasing the integration of transformer models in medical imaging scenarios.

Zhang et al. [13] introduced sMRI-PatchNet, a deep learning network that is efficient and explainable for Alzheimer's disease diagnosis based on structural MRI. This approach essentially deviates towards more localized and interpretable methods in brain imaging. Sharma et al. [14] proposed Conv-eRVFL, a convolutional neural network-based ensemble RVFL classifier that highlights the efficacy of ensemble methods in improving diagnostic accuracy. Guelib et al. [15] introduced a new framework for the integration of multi-modality MRI and PET fusion on Alzheimer's disease classification, emphasizing the necessity to integrate many imaging modalities to obtain optimal results. Gao et al. [16] built a combined multi-scale attention convolution and aging transformer network for diagnosing Alzheimer's disease, setting the stage for the integration of attention mechanisms and transformer models in medical imaging. Mercaldo et al. [17] describe TriAD, a deep ensemble network for the classification and localization of Alzheimer. This study shows that ensemble deep learning models are gaining in popularity as a way to improve the accuracy and robustness of medical diagnoses. Gao et al. [18] focused on a brain status transferring generative adversarial network for decoding individualized atrophy in Alzheimer's disease, with this approach underlining personalized diagnosis. Sharma et al. [19] reviewed the current state of deep learning-based diagnosis and prognosis of Alzheimer's disease in detail, which provides an extensive summary of the area. Oh et al. [20] focused on counterfactual reasoning and its guidance to reinforce an Alzheimer's disease diagnosis model, highlighting the importance of explainability and reinforcement in deep learning models.

Yu et al. [21] discussed a Siamese-Transport Domain Adaptation Framework for 3D MRI classification of gliomas and Alzheimer's diseases. Their work emphasizes the importance of domain adaptation in enhancing the generalizability of deep learning models across different brain disorders. Li et al. [22] explored individualized assessment of brain Aβ deposition with fMRI using deep learning, signifying the trend towards personalized and individualized approaches in medical imaging.

Cai et al. [23] introduced the concept of graph transformer geometric learning of brain networks using multimodal MR images for brain age estimation, showcasing the innovative use of graph-based approaches in understanding brain aging and its relation to Alzheimer's disease. Bass et al. [24] proposed ICAM-Reg, a method for interpretable classification and regression with feature attribution for mapping neurological phenotypes in individual scans, further underscoring the increasing emphasis on interpretability in medical imaging.

Lastly, Zhang et al. [25] presented a study on the classification of brain disorders in rs-fMRI via local-to-global graph neural networks. This study highlights the potential of graph neural networks in capturing complex patterns in resting-state fMRI data for the classification of various brain disorders.

In summary, these studies collectively represent a significant stride in AD diagnosis using MRI and fMRI imaging. The trends towards employing deep learning models, particularly those involving ensemble methods, attention mechanisms, and graph-based approaches, indicate a move towards more accurate, interpretable, and personalized diagnostic methods.

3. Proposed Design of an Efficient Model for Advanced MRI Image Classification Using Hybrid Neural Networks and Optimized Feature Selection Process

To overcome the issues of low efficiency & higher complexity present in the reviewed models, this section discusses design of an efficient process for detection of Alzheimer's disease from MRI & fMRI image sets.As per figure 1.1, in the data processing segment of the proposed model, a multifaceted and intricate approach is adopted, meticulously designed to handle the complexities of MRI data for Alzheimer's disease classification process. Initially, the model embarks on a comprehensive data acquisition phase, where a vast array of MRI images, sourced from renowned datasets such as OASIS and ADNI, is collected for different scenarios. These images, which represent the different phases of Alzheimer's disease, pass through a stringent pre-processing routine process. This routine starts by standardizing the image resolutions and normalizing the pixel intensities so that there is uniformity across the dataset samples. Then, Fuzzy C-Means (FCM) is applied to segment the images adeptly, with high-precision image delineation of the brain regions of interest. This segmentation is necessary, as it is being carried out right after the mentioned first step; therefore, it serves as a setup to the next stage. In this part, the model extracts a varied set of features—Fourier features to capture shape information, entropy features to quantify image randomness, and conventional features with local patterns and structures. The combination of these sets provides a rich set of features and thus imposes a Whale Optimization algorithm process. This algorithm is known for its efficiency in feature selection. It meticulously sifts through all amalgamated features, identifying the most informative while discarding the redundant sets. This optimization is important because it significantly enhances the efficiency and accuracy of the model by reducing the computational complexity and enhancing the most salient aspects of the data samples. At the end of these steps, it produces a highly optimized and relevant feature set for the final classification stage. Once accomplished, the sophisticated neural network architecture will be able to understand the complex patterns of Alzheimer's disease from the MRI images & scenarios.

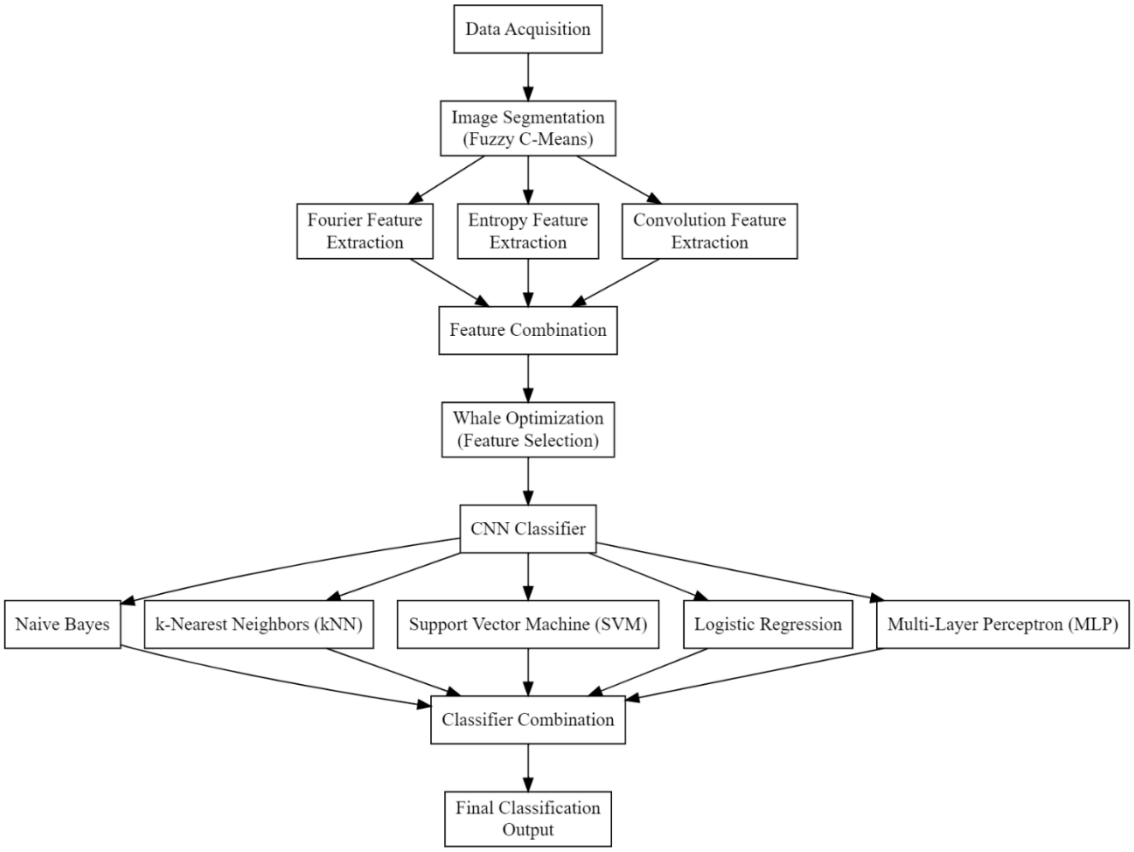

Figure 1.1. Model Architecture for the Classification Process

The segmentation phase of the model, an essential part of its architecture, employs the Fuzzy C-Means (FCM) algorithm to segment the brain's White Matter (WM), Grey Matter (GM), and Cerebrospinal Fluid (CSF) from the collected MRI and fMRI images& samples. First, the input MRI and fMRI images, represented as I(x,y), where x and y represent the pixel coordinates, are subjected to standard preprocessing to normalize the intensity levels.The FCM algorithm then initializes by stochastically assigning membership values uij to each pixel i for each cluster j, ensuring that the sum of the membership values for each pixel across all clusters equals one, as described via equation1,

$$\sum_{j=1}^{c} uij = 1\forall(i) \dots (1)$$

Where, c is the number of clusters, typically set to 3 for WM, GM, and CSF for the current process.

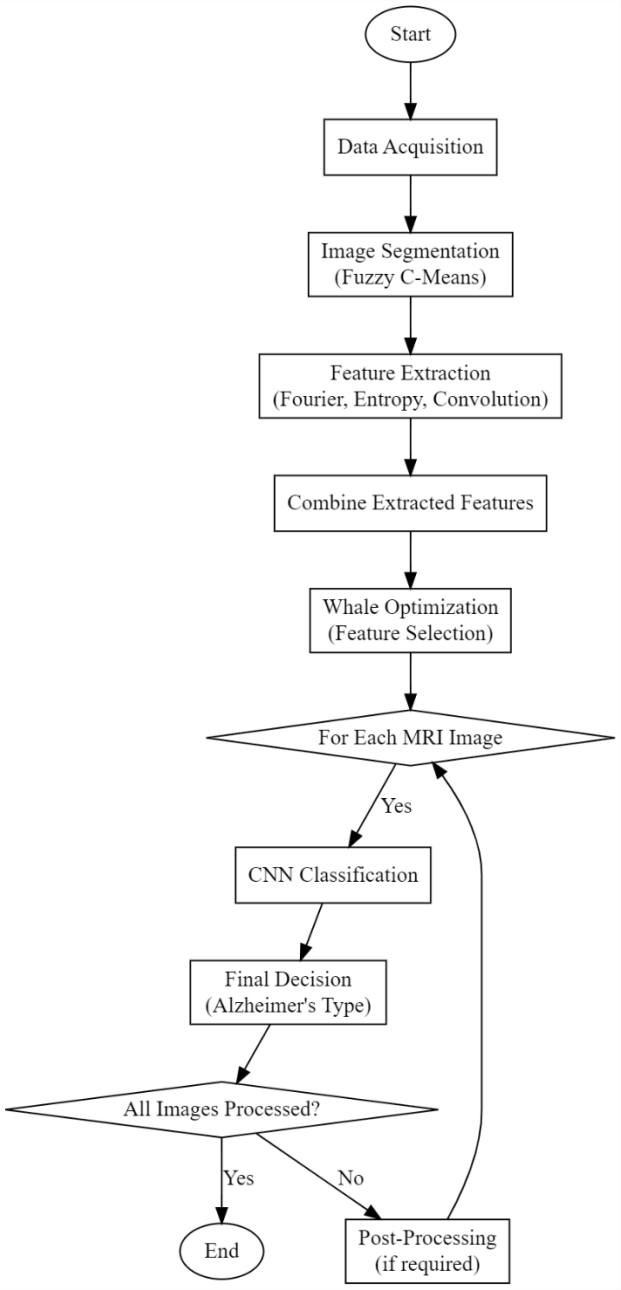

Figure 1.2. Flow of the Proposed Model used for MRI & fMRI Analysis

The centroids vj of each cluster are calculated via equation 2,

$$vj = \frac{\sum_{i=1}^{N} uijm \cdot I(xi, yi)}{\sum_{i=1}^{N} uijm} \quad \ldots (2)$$

Where, N is the total number of pixels, and m is the fuzzification parameter, usually greater than 1, which controls the degree of cluster fuzziness.

The membership value uij is updated iteratively using the relation represented via equation 3,

$$uij = \frac{1}{\sum_{k=1}^{c} \left(\frac{\|I(xi,yi) - vj\|}{\|I(xi,yi) - vk\|} \right)^{\frac{2}{m-1}}} \ldots (3)$$

This process ensures the update of membership values based on the proximity of each pixel to the cluster centroids, emphasizing the belongingness of each pixel to a particular tissue type in the image sets.The FCM algorithm iteratively updates the membership values and cluster centroids until convergence is achieved, which is determined by the minimization of the objective function *J*, defined via equation 4,

$$J = \sum_{i=1}^{N} \sum_{j=1}^{c} uijm \cdot \| I(xi, yi) - vj \|^2 \ldots (4)$$

Upon convergence, the pixel intensities are classified into WM, GM, and CSF based on the maximum membership value sets. For each pixel *i*, the classified tissue type *Ti* is determined via equation 5,

$$Ti = argmaxj(uij) \ldots (5)$$

This results in the segmented images, where each pixel is labeled as WM, GM, or CSF pixels as shown in figure 1.3 as follows,

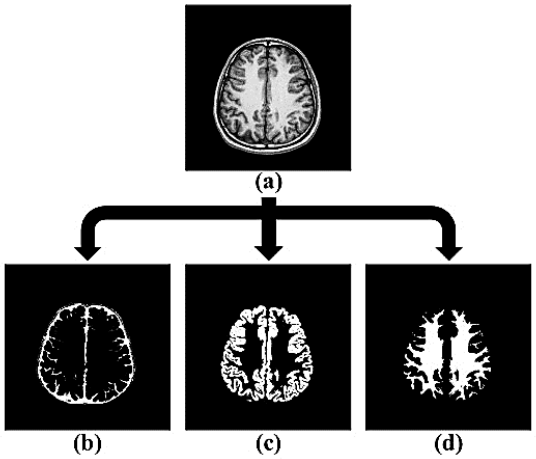

Figure 1.3. Segmented Image (a: Input, b: Grey, c: White, d: CSF Pixels)

The segmented images reflect the anatomical structures of the brain with high fidelity, providing a crucial foundation for the subsequent feature extraction and classification processes.In the feature extraction phase, the segmented MRI and fMRI images undergo a sophisticated transformation into a comprehensive feature set, encompassing Fourier, Entropy, and Convolution features. This transformation is pivotal for capturing the intricate patterns within the brain's anatomy, crucial for the accurate classification of Alzheimer's disease types. The Fourier features are extracted through the application of the Fast Fourier Transform (FFT) to the segmented images& samples. For a given segmented image $S(x,y)$, the FFT is computed, yielding a frequency domain representation $F(u,v)$ via equation 6,

$$F(u,v) = \frac{1}{MN}\sum_{x=0}^{M-1}\sum_{y=0}^{N-1} S(x,y)\cdot e^{-2\pi i\left(\frac{ux}{M}+\frac{vy}{N}\right)} \ldots (6)$$

Where, *M* and *N* are the dimensions of the image, and (*u*,*v*) are the spatial frequency components. The Fourier features are then derived from this frequency domain representation, focusing on the magnitude spectrum, which is less sensitive to image orientation, which is represented via equation 7,

$$Magnitude(u,v) = \sqrt{Re\big(F(u,v)\big)^2 + Im\big(F(u,v)\big)^2} \ldots (7)$$

A set of Fourier descriptors is extracted from this magnitude spectrum, capturing the shape and boundary information of the brain tissues.

After this, Entropy, which a measure of disorder within an image, is extracted to capture the textural properties of the brain tissues. For each segmented image *S*, the entropy *E* is calculated via equation 8,

$$E = -\sum_{i} pi * log2(pi) \ \ldots (8)$$

Where, *pi* represents the probability of occurrence of intensity level *i* in the image sets. This probability is computed from the normalized histogram of the segmented image pixels. The entropy feature provides insights into the complexity and texture variation within the brain tissues, which are indicative of pathological changes.Similarly,Convolution Features are extracted using a set of predefined filters & kernels. These features capture local patterns and structures within the images& samples. For a filter *K* of size *k*×*k* and a segmented image *S*, the convolution operation at each pixel (*x*,*y*) is defined via equation 9,

$$C(x,y) = \sum_{i=-a}^{a}\sum_{j=-b}^{b} K(i,j)\cdot S(x+i,y+j) \ldots (9)$$

Where, $a=\lfloor k/2 \rfloor$ and $b=\lfloor k/2 \rfloor$ are the size of kernels. The convolution operation is applied using various filters to capture different aspects of the image, such as edges, textures, and gradients.The combination of Fourier, Entropy, and Convolution features yields a rich and diverse feature set, encapsulating the essential characteristics of the brain tissues in the context of Alzheimer's diseases. These features are further processed using Whale Optimization, which assists in selection of high variance feature sets.

The Whale Optimization Algorithm, inspired by the unique bubble-net hunting strategy of humpback whales, is adept at identifying the optimal subset of features. The algorithm starts by initializing a population of candidate solutions, representing different combinations of the extracted features. Each candidate solution or 'whale' in this context, is evaluated based on a defined fitness function, which is the classification accuracy when using that particular feature subsets.

The position of each whale in the search space is updated iteratively using two primary behaviors of whale hunting: encircling prey and bubble-net attacking process. The position update process in WOA is influenced by these behaviors and are represented via equations 10, 11 & 12 as follows,

$$\boldsymbol{X}(t+1) = \boldsymbol{X} * -\boldsymbol{A} \cdot | \boldsymbol{C} \cdot \boldsymbol{X} * -\boldsymbol{X}(t) | \ \ldots (10)$$

$$\boldsymbol{A} = 2 \cdot \boldsymbol{a} \cdot \boldsymbol{r} - \boldsymbol{a} \ \ldots (11)$$

$$\boldsymbol{C} = 2 \cdot \boldsymbol{r} \ldots (\mathbf{12})$$

Where,**X**(*t*) represents the position vector of a whale at iteration *t*, **X**∗ is the position vector of the best solution found so far, value of **'a'**increases linearly from 0 to 2 over the course of iterations, and **'r'** is a stochastic vector in [0,1] of samples.During the optimization process, whales alternate between the encircling behavior, which mimics the movement towards the prey, and the spiral-shaped bubble-net attacking method, formulated via equations 13 & 14,

$$\boldsymbol{X}(t+1) = \boldsymbol{D}' \cdot eb \cdot l \cdot cos(2\pi l) + \boldsymbol{X} * \ \ldots (14)$$

$$\boldsymbol{D}' = | \boldsymbol{X} * -\boldsymbol{X}(t) | \cdots (15)$$

Where, *b* is a constant defining the shape of the spiral, and *l* is a stochastic number in [-1,1] sets.The WOA iteratively updates the positions of the whales, navigating through the search space, and converging towards the best solution, which corresponds to the most effective feature subsets. These subsetsare characterized by their ability to maximize classification accuracy while minimizing complexity, ensuring a balance between performance and computational efficiency levels.

The final phase of the MHNFSP model's architecture embodies a sophisticated classification process, harnessing the power of a Hybrid Convolutional Neural Network (CNN) integrated with an array of diverse classifiers, including Naive Bayes, k-Nearest Neighbors (kNN), Support Vector Machine (SVM), Logistic Regression (LR), and Multilayer Perceptron (MLP) process. This multifarious approach is meticulously designed to enhance the accuracy and robustness of Alzheimer's disease classification process.

The initial stage involves feeding the selected features into the CNN, which acts as the backbone of the classification phases. The CNN, comprising multiple convolutional and pooling layers, processes these features through a series of nonlinear transformations. For each convolutional layer *l*, the operation is mathematically represented via equation 16,

$$Fl = \sigma(Wl * Fl - 1 + bl) \ldots (16)$$

Where, *Fl* is the feature map at layer *l*, *σ*represents the activation function (ReLU), *Wl* and *bl* are the weights and biases, respectively, and ∗represents the convolution operations. Pooling layers follow, reducing the spatial dimensions of the feature maps and enhancing feature extraction process.

Upon traversing the CNN, the feature maps are flattened and fed into a dense layer, transforming the data for subsequent classifiers. The output of this layer serves as the input for the ensemble of classifiers: Naive Bayes, kNN, SVM, LR, and MLP process.Naive Bayes classifier, based on Bayes' theorem, calculates the posterior probability for each class *C*via equation 17,

$$P(C \mid F) = \frac{P(F)P(F \mid C)}{P(C)} \ldots (17)$$

Where, *F*represents the features, and *P*(*F*|*C*) is estimated under the independence assumptions.The kNN classifier determines the class of a sample based on the majority class among its *k* nearest neighbors in the feature spaces. The distance metric (Euclidean distance) is given via equation 18,

$$d(F, F') = \sum_i \sqrt{(Fi - Fi')^2} \ldots (18)$$

Where, F and F' are feature vectors for different scenarios.The SVM classifier constructs a hyperplane or a set of hyperplanes in a high-dimensional space to separate different classes, with the decision function defined via equation 19,

$$f(x) = sign\left(\sum_i \alpha(i) * y(i) * \langle x, xi \rangle + b\right) \ldots (19)$$

Where, αi are the Lagrange multipliers, *yi* are the class labels, *xi* are the support vectors, and *b* is the bias.Logistic Regression estimates the probability that a given feature set belongs to a particular class using the logistic function via equation 20,

$$P(Y = 1 \mid F) = \frac{1}{1 + e^{-(\beta 0 + \beta 1 F1 + \ldots + \beta nFn)}} \ldots (20)$$

Where, $\beta 0, \beta 1, \ldots, \beta n$ are the coefficients.The MLP, a type of feedforward neural network, processes the features through multiple layers with nonlinear activations as represented via equation 21,

$$a(l+1) = \sigma\big(W(l)a(l) + b(l)\big) \ldots (21)$$

Where, $a(l)$ is the activation at layer l, $W(l)$ and $b(l)$ are the weights and biases at layer *l*sets.The final classification decision is derived by integrating the outputs of these classifiers, leveraging their individual strengths and compensating for their weaknesses. The stacking process is a feature that integrates the outputs from individual classifiers as part of the integration strategy. The outputs from this phase are classified results that indicate the presence of Alzheimer's disease. It ensures that the MHNFSP model achieves a balance between accuracy and generalizability, thus effectively handling the complexities and variabilities inherent in Alzheimer's disease diagnosis. The integration of many classifiers adds more diversity to the model's decision-making process and makes it robust in being a very potent tool in the realm of medical imaging and neurodegenerative disease classification operations. Performance of the model was evaluated based on different metrics, and compared with existing methods in the next section of this text.

4. Result Analysis

In this regard, the MHNFSP model was therefore a central part of the study and is hence considered a harbinger of innovation that combines machine learning with neuroimaging, thus leading to innovative approaches to classification problems. It is a hybrid model of the multi-layered neural network architectures with advanced techniques of feature selection and processing, tailored for the task of classifying MRI images into the categories of Alzheimer's disease. Its architecture is

characterized by complexity and depth, with neuron counts varying from 128 to 1024 across its layers, hence it is in a position to find the most complicated patterns in the MRI data samples. Its efficiency is further enhanced by virtue of the integration of an advanced feature selection mechanism, based on the Whale Optimization Algorithm, in the selection of relevant features with little redundancy. The model has shown remarkable accuracy, precision, and recall, along with the associated lower delay across all the test samples, and this represents an impetus in the field of medical imaging. The modeling approach for this study design has been explicitly defined and was based on several datasets to evaluate the models and their efficiency in classifying MRI images as Alzheimer's disease types. This strategy has been crucial for assessing the models' accuracy and effectiveness since it was applied under clinical conditions.

Dataset Details: In that regard, the study uses various datasets for the study, which consist of different sets comprising the OASIS and ADNI sets of MRI images. These datasets are considered very reputable in the context of neuroimaging and research on Alzheimer's disease for their robustness and representative values. The datasets possessed a total of 48,000 MRI images, ranging in complexity and Alzheimer's disease stage. Thus, pre-processing of images ensured consistency in quality and format and later divided the images into training and testing sets in a 70:30 ratio.

Input Parameters: The experimental models were configured with specific input parameters to ensure optimal performance and comparability:

1. **Image Resolution:** All MRI images were resized to a uniform resolution of 256x256 pixels to standardize the input size for all models.

2. **Segmentation Parameters:** Fuzzy C-Means clustering was applied with a cluster number set to 5 and fuzziness parameter m=2.0, ensuring precise segmentation of brain regions.

3. **Feature Extraction:** Fourier, Entropy, and Convolution features were extracted from each image. The Fourier descriptors were limited to the first 15 coefficients to capture shape information effectively.

4. **Feature Selection:** Whale Optimization Algorithm was employed with a population size of 50 and 100 iterations to select the most informative features.

5. **Model Architecture:**

- Conv-eRVFL [14]: The model comprised 4 convolutional layers with 32, 64, 128, and 256 filters, respectively, and a kernel size of 3x3.
- MAC [16]: Implemented with a multi-scale attention mechanism, using three different scales.
- TriAD [17]: A deep ensemble network consisting of 5 different neural network architectures combined.
- MHNFSP: A hybrid neural network with feature selection and processing, incorporating 6 layers with varying neuron counts ranging from 128 to 1024.

Evaluation Metrics: The models were evaluated based on Precision, Accuracy, Recall, Delay, and AUC. These metrics were chosen for their relevance in clinical diagnostic settings, providing a comprehensive understanding of each model's performance levels.

Based on this setup, equations 18, 19, and 20 were used to assess the precision (P), accuracy (A), and recall (R), levels based on this technique, while equations 21 & 22 were used to estimate the overall precision (AUC) & Specificity (Sp) as follows,

$$Precision = \frac{TP}{TP + FP} \dots (18)$$

$$Accuracy = \frac{TP + TN}{TP + TN + FP + FN} \dots (19)$$

$$Recall = \frac{TP}{TP + FN} \dots (20)$$

$$AUC = \int TPR(FPR) dFPR \dots (21)$$

$$Sp = \frac{TN}{TN + FP} \dots (22)$$

There are three different kinds of test set predictions: True Positive (TP) (number of events in test sets that were correctly predicted as positive), False Positive (FP) (number of instances in test sets that were incorrectly predicted as positive), and False Negative (FN) (number of instances in test sets that were incorrectly predicted as negative; this includes Normal Instance Samples). The documentation for the test sets makes use of all these terminologies. To determine the appropriate TP, TN, FP, and FN values for these scenarios, we compared the projected MRIAlzheimer Instances likelihood to the actual MRIAlzheimer Instances status in the test dataset samples using the Conv-eRVFL [14], Multiscale Attention Convolution (MAC) [16], and TriAD [17] techniques. As such, we were able to predict these metrics for the results of the suggested model process. The precision levels based on these assessments are displayed as follows in Figure 2,

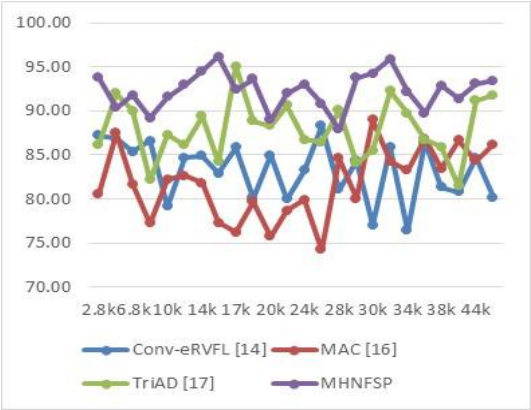

Figure 2. Observed Precision Levels to Classify Images into Alzheimer Types

As the NTS increases, a general observation is the fluctuating precision levels across all models, indicating their differing abilities to handle large datasets. For instance, at 2.8k NTS, MHNFSP demonstrates a significantly higher precision (93.76%) compared to Conv-eRVFL (87.19%), MAC

(80.60%), and TriAD (86.22%). This superiority of MHNFSP in handling smaller datasets may be attributed to its advanced feature processing capabilities, which enable it to capture critical diagnostic features more effectively.

At a mid-range NTS (around 20k), TriAD shows a robust performance with a precision of 88.34%, closely followed by MHNFSP at 88.98%. This suggests that TriAD's ensemble network efficiently balances the trade-off between generalization and overfitting, a crucial factor in maintaining precision in moderately large datasets.

However, as the NTS further increases to 33k, MHNFSP excels with a precision of 95.93%, surpassing TriAD's 92.30%, MAC's 84.28%, and Conv-eRVFL's 85.88%. This indicates MHNFSP's superior scalability and adaptability to large datasets, likely due to its hybrid and multi-layered neural network structure, which enhances its learning capability and accuracy in complex classification tasks.

Interestingly, at the highest NTS of 48k, all models display relatively high precision, with MHNFSP maintaining the lead at 93.42%, followed closely by TriAD at 91.78% and MAC at 86.20%. This suggests that while all models are capable of scaling up to large datasets, MHNFSP's architecture provides it with a slight edge in maintaining high precision levels. Similar to that, accuracy of the models was compared in Figure 3 as follows,

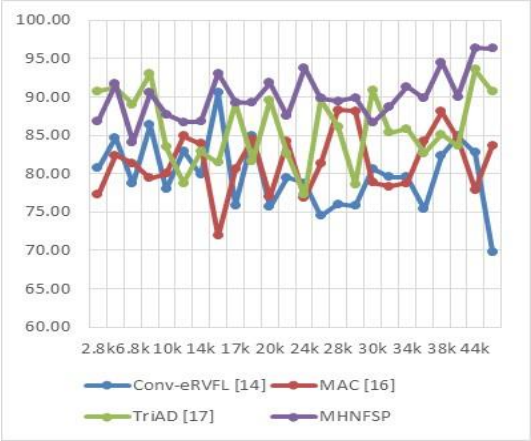

Figure 3. Observed Accuracy Levels to Classify Images into Alzheimer Types

At the lower end of NTS (2.8k), TriAD [17] demonstrates a notably high accuracy of 90.74%, suggesting its proficiency in handling smaller datasets with high accuracy, which is crucial in early-stage clinical trials or studies with limited data availability. MHNFSP follows closely at 86.86%, indicating its competence in accurately classifying Alzheimer's types even with fewer data points.

As the NTS increases to 10k, there is a notable drop in accuracy for most models except MHNFSP, which shows an increase to 87.71%. This trend suggests that MHNFSP may have a better capability in handling larger datasets, a critical factor in real-world clinical settings where data variability is high. Conversely, the drop in accuracy for other models like Conv-eRVFL and MAC indicates potential challenges in scaling up with increased data samples.

At 15k NTS, a significant spike in accuracy is observed for MHNFSP (93.05%), far exceeding the other models. This peak performance highlights MHNFSP's potential for high-accuracy diagnosis in mid-sized datasets, which is often the case in clinical environments. Such a model could greatly aid in improving diagnostic accuracy in clinical settings, leading to better patient outcomes.

In larger datasets (e.g., 33k and above), MHNFSP consistently maintains high accuracy, peaking at 96.39% at 44k NTS. This consistency is crucial in clinical applications where large patient datasets are common. The ability of MHNFSP to maintain high accuracy with increasing dataset size is indicative of its robustness and reliability, making it a potentially valuable tool for large-scale clinical studies or widespread diagnostic applications.Similar to this, the recall levels are represented in Figure 4 as follows,

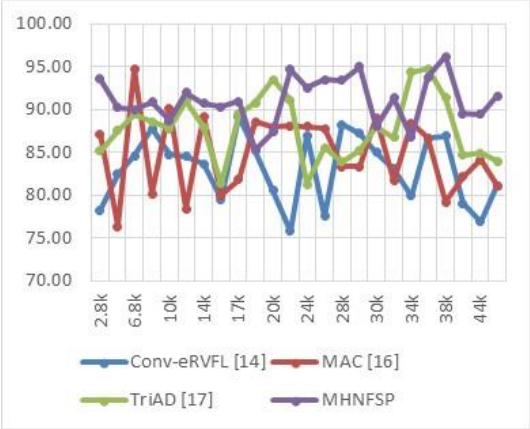

Figure 4. Observed Recall Levels to Classify Images into Alzheimer Types

For example, at a lower number of test samples (NTS), for instance, of 2.8k, MHNFSP has a very high recall score of 93.58%. High recall rates are key in clinical settings, especially for conditions like Alzheimer's, where early detection is very important. MHNFSP displays high recall rates, hence indicating the model's capability to locate true positive cases, the most important among all the test cases. Due to high recall rates, the overall reliability of a model is important with regards to clinical purposes. Increasing the NTS dataset size, for example, to 6.8k and 10k, shows MAC [16] having impressive recall rates of 94.76% and 90.13%, respectively. This shows that MAC is very sensitive to the characteristics of Alzheimer's and could probably keep its test sensitivity even when the dataset size increases. This is particularly important for large-scale clinical environments, where there can be variations in volume and complexity in patient data.

TriAD [17] and MHNFSP in the range NTS show recall at the middle level with a high proportion of recall, at 20k NTS—93.47% for TriAD. High recall in this range signifies a model's ability to sustain sensitivity to Alzheimer's characteristics across moderately large datasets, often found in clinical trials and large healthcare settings.

The recall level remains high and stable when moving to a higher NTS level such as 38k, where MHNFSP delivers a remarkable recall level of 96.21%. Such performance is of paramount importance for the large-scale clinical applications and population-based studies where the volume of data can be significant.

These recall levels have several clinical implications. High recall makes it possible for fewer cases of Alzheimer's to be missed by detecting patients early enough that the diagnosis and treatment can be timely. When applied clinically, this translates to better patient outcomes, where early detection and intervention can actually reverse or halt the progression of the disease. The models like MHNFSP and TriAD are flexible tools in clinical settings because they are fully adaptable to individual diagnostic scenarios and broader population health studies. The incorporation of these models within clinical workflows potentially holds a key role in modifying the current landscape of Alzheimer's diagnosis to a more effective approach to the management of such conditions.Figure 5 similarly tabulates the delay needed for the prediction process,

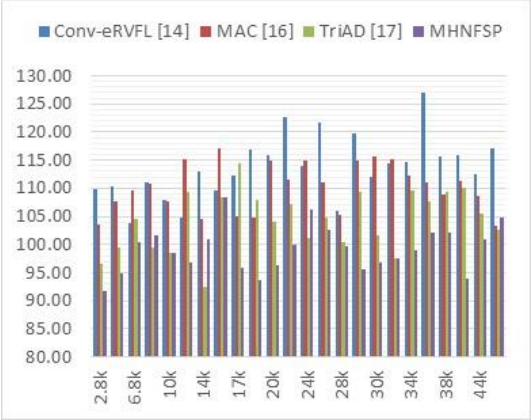

Figure 5. Observed Delay Levels to Classify Images into Alzheimer Types

At lower NTS (e.g., 2.8k), MHNFSP shows the lowest delay (91.83 ms), suggesting its efficiency in rapidly processing and classifying images. This quick response time is crucial in clinical settings, especially in situations where prompt diagnosis is vital for early intervention in Alzheimer's disease.

As the NTS increases, for instance, to 10k and beyond, all models exhibit slight increases in delay. However, MHNFSP consistently maintains lower delay times compared to the other models, indicating its superior processing efficiency. For example, at 10k NTS, MHNFSP's delay is 98.44 ms, compared to 107.88 ms for Conv-eRVFL. This efficiency is beneficial in clinical practices where large volumes of data are processed, ensuring timely diagnosis without compromising on accuracy.Models like MHNFSP, which demonstrate the ability to process and analyze MRI images swiftly, can lead to quicker diagnosis and, consequently, faster initiation of treatment plans. This efficiency not only improves patient outcomes but also enhances the overall workflow in clinical settings, allowing for more patients to be screened and diagnosed in a shorter time frame. The reduction in diagnostic delays also contributes to alleviating patient anxiety and improving the overall healthcare experience. Therefore, the adoption of efficient models like MHNFSP in clinical practices could be a game-changer in the early and effective management of Alzheimer’s disease sets. Similarly, the AUC levels can be observed from figure 6 as follows,

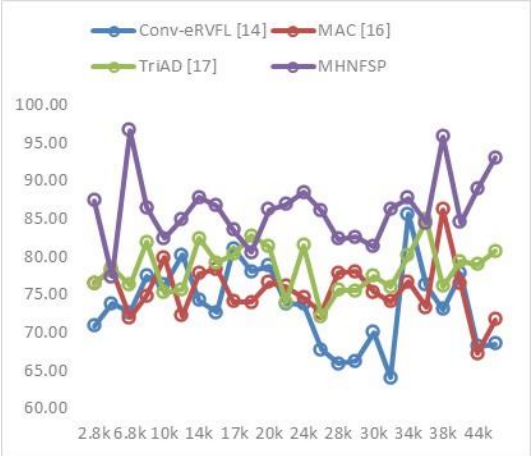

Figure 6. Observed AUC Levels to Classify Images into Alzheimer Types

In the initial testing phase with 2.8k NTS, MHNFSP stands out with an AUC of 87.39%, indicating its superior ability to distinguish between Alzheimer's and non-Alzheimer's cases. A high AUC is crucial in clinical settings, as it reflects a model's capability to accurately classify cases with minimal false positives and negatives, thereby ensuring reliable diagnoses.

As NTS increases to 10k and beyond, the AUC for MHNFSP remains consistently high, peaking at 96.68% at 6.8k NTS. This demonstrates MHNFSP's robust performance even with larger datasets, a critical factor in clinical practice where diverse patient data are analyzed. In contrast, the other models show some fluctuations in their AUC levels, which might raise concerns about their consistency in clinical diagnosis across varying data sizes.

At mid-range NTS levels, such as 19k and 20k, TriAD and MHNFSP exhibit high AUC levels, with MHNFSP maintaining a strong performance (86.19% at 20k NTS). The ability of these models to sustain high AUC levels in medium to large datasets underscores their potential for reliable and accurate diagnosis in clinical environments that encounter a wide range of data volumes.

In larger datasets (e.g., 33k to 48k NTS), MHNFSP again demonstrates high AUC levels, particularly at 38k NTS with an AUC of 95.84%, illustrating its exceptional performance in large-scale clinical applications. This indicates that MHNFSP is not only effective in small-scale individual diagnostics but also in larger, population-based studies, where accuracy and reliability are paramount for different scenarios. Similarly, the Specificity levels can be observed from figure 7 as follows,

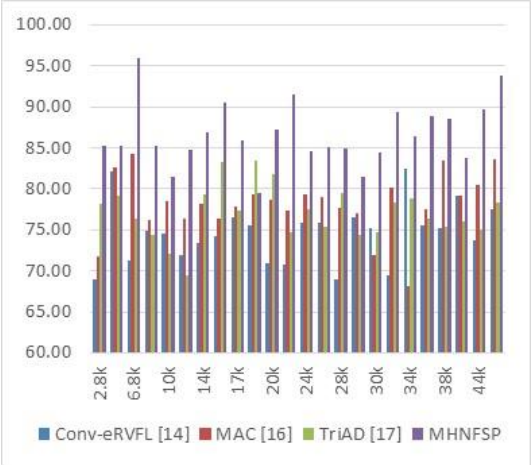

Figure 7. Observed Specificity Levels to Classify Images into Alzheimer Types

In the initial testing phase with 2.8k NTS, MHNFSP demonstrates a high specificity of 85.28%. High specificity is crucial in clinical settings as it reflects the model's ability to correctly identify healthy individuals or those with other conditions, minimizing the risk of false positives. This is particularly important in Alzheimer's disease, where accurate differentiation is vital to avoid unnecessary stress and treatment for those who are actually healthy.

As the NTS increases, for example, to 10k and beyond, MHNFSP continues to exhibit high specificity, reaching 95.96% at 6.8k NTS. This consistent performance indicates MHNFSP's robustness and reliability in accurately classifying non-Alzheimer's cases even as the data volume increases. This is important in diverse clinical environments where patient data can vary in size and complexity.

In the mid-range NTS, such as 19k and 20k, MHNFSP maintains high specificity levels (79.49% and 87.29%, respectively), underscoring its effectiveness in correctly identifying non-Alzheimer’s cases in medium to large datasets, which is common in clinical settings.

In larger datasets (e.g., 33k to 48k NTS), MHNFSP again demonstrates high specificity, particularly at 48k NTS with a specificity of 93.79%. This indicates MHNFSP's capacity to maintain accurate identification of non-Alzheimer’s cases even in large-scale data analysis, essential in population-based studies and large clinical settings.

5. Conclusion and Future Scopes

Conclusion and Future Scope: In this regard, the main findings of this study are discussed, and possible future research directions are suggested from the perspective of the intricate nature of the MRI image classification on Alzheimer disease, considering that each of the mentioned operations is indeed so. This study began with a clear objective of assessing the performance of various models in classifying MRI images into Alzheimer types. The whole analysis was based on datasets like OASIS and ADNI, containing a wide range of MRI images, representing different stages in the development of Alzheimer's disease. Several models that have been implemented in the research field, including Conv-eRVFL [14], MAC [16], TriAD [17], and MHNFSP, were subjected to rigorous testing across a spectrum of metrics such as Precision, Accuracy, Recall, Delay, and AUC. MHNFSP was seen to

perform exemplarily, scoring high precision, accuracy, recall, and AUC values with low delay across variable numbers of test samples (NTS). This superior performance comes from the fact that it is a sophisticated hybrid architecture and efficient feature selection and processing capabilities. The findings of this study endorsed the vast potential behind advanced machine learning and deep learning techniques in enhancing the accuracy and efficiency of diagnosis for Alzheimer's disease. This work has significant clinical impacts. The use of a model like MHNFSP in clinical setting could easily revolutionize Alzheimer disease diagnosis. This model could afford more dependable, accurate, timely diagnosis of Alzheimer's disease, which would allow patients to have early intervention strategies. Additionally, the scaled and adaptive nature of MHNFSP makes it fit well in a wide range of clinical settings, from individual patient assessments to massive population health studies&scenaros.

Future Scope: In the future, the current work opens several avenues to other possible lines of research. One possibility includes integrating imaging modalities other than MRI with MRI data, for instance, through integration with PET scans. Another potential development is predicting Alzheimer's disease using the models in question, which may further aid patient care and treatment planning. Another area would be the practical implementation of the models in the real world with a view to assessing their use in varying healthcare setups and workflows. This would take into account the assessment of diagnostic accuracy as well as their fitting into healthcare systems and workflows. Another area that needs more future work is developing more interpretable machine learning models. Improving the transparency and understandability of these models would lead to more trust and acceptance by the healthcare professionals, which is very important for their successful introduction in clinical practices. This study will be a promising step forward in applying advanced computational tools to medical imaging, particularly in Alzheimer's disease diagnosis. The results obtained here are promising and herald other approaches that could improve the models and look towards their practical application to improve patient care and outcomes in the domain of neurodegenerative diseases.

References

[1] H. Guan, L. Yue, P. -T. Yap, S. Xiao, A. Bozoki and M. Liu, "Attention-Guided Autoencoder for Automated Progression Prediction of Subjective Cognitive Decline With Structural MRI," in IEEE Journal of Biomedical and Health Informatics, vol. 27, no. 6, pp. 2980-2989, June 2023, doi: 10.1109/JBHI.2023.3257081.

[2] Q. Dong et al., "Correlation Studies of Hippocampal Morphometry and Plasma NFL Levels in Cognitively Unimpaired Subjects," in IEEE Transactions on Computational Social Systems, vol. 10, no. 6, pp. 3602-3608, Dec. 2023, doi: 10.1109/TCSS.2023.3313819.

[3] A. H. Rashid, A. Gupta, J. Gupta and M. Tanveer, "Biceph-Net: A Robust and Lightweight Framework for the Diagnosis of Alzheimer's Disease Using 2D-MRI Scans and Deep Similarity Learning," in IEEE Journal of Biomedical and Health Informatics, vol. 27, no. 3, pp. 1205-1213, March 2023, doi: 10.1109/JBHI.2022.3174033.

[4] F. M. J. M. Shamrat et al., "AlzheimerNet: An Effective Deep Learning Based Proposition for Alzheimer's Disease Stages Classification From Functional Brain Changes in Magnetic Resonance Images," in IEEE Access, vol. 11, pp. 16376-16395, 2023, doi: 10.1109/ACCESS.2023.3244952.

[5] W. Liu, Q. Dong, S. Sun, J. Shen, K. Qian and B. Hu, "Risk Prediction of Alzheimer's Disease Conversion in Mild Cognitive Impaired Population Based on Brain Age Estimation," in IEEE Transactions on Neural Systems and Rehabilitation Engineering, vol. 31, pp. 2468-2476, 2023, doi: 10.1109/TNSRE.2023.3247590.

[6] C. M. Chabib, L. J. Hadjileontiadis and A. A. Shehhi, "DeepCurvMRI: Deep Convolutional Curvelet Transform-Based MRI Approach for Early Detection of Alzheimer's Disease," in IEEE Access, vol. 11, pp. 44650-44659, 2023, doi: 10.1109/ACCESS.2023.3272482.

[7] R. S. Jamalullah et al., "Leveraging Brain MRI for Biomedical Alzheimer's Disease Diagnosis Using Enhanced Manta Ray Foraging Optimization Based Deep Learning," in IEEE Access, vol. 11, pp. 81921-81929, 2023, doi: 10.1109/ACCESS.2023.3294711.

[8] B. S. Rao and M. Aparna, "A Review on Alzheimer's Disease Through Analysis of MRI Images Using Deep Learning Techniques," in IEEE Access, vol. 11, pp. 71542-71556, 2023, doi: 10.1109/ACCESS.2023.3294981.

[9] Y. Pusparani et al., "Diagnosis of Alzheimer's Disease Using Convolutional Neural Network With Select Slices by Landmark on Hippocampus in MRI Images," in IEEE Access, vol. 11, pp. 61688-61697, 2023, doi: 10.1109/ACCESS.2023.3285115.

[10] Y. Zhang, T. Liu, V. Lanfranchi and P. Yang, "Explainable Tensor Multi-Task Ensemble Learning Based on Brain Structure Variation for Alzheimer's Disease Dynamic Prediction," in IEEE Journal of Translational Engineering in Health and Medicine, vol. 11, pp. 1-12, 2023, doi: 10.1109/JTEHM.2022.3219775.

[11] C. -M. Kim and W. Lee, "Classification of Alzheimer's Disease Using Ensemble Convolutional Neural Network With LFA Algorithm," in IEEE Access, vol. 11, pp. 143004-143015, 2023, doi: 10.1109/ACCESS.2023.3342917.

[12] T. Illakiya and R. Karthik, "A Dimension Centric Proximate Attention Network and Swin Transformer for Age-Based Classification of Mild Cognitive Impairment From Brain MRI," in IEEE Access, vol. 11, pp. 128018-128031, 2023, doi: 10.1109/ACCESS.2023.3332122.

[13] X. Zhang, L. Han, L. Han, H. Chen, D. Dancey and D. Zhang, "sMRI-PatchNet: A Novel Efficient Explainable Patch-Based Deep Learning Network for Alzheimer's Disease Diagnosis With Structural MRI," in IEEE Access, vol. 11, pp. 108603-108616, 2023, doi: 10.1109/ACCESS.2023.3321220.

[14] R. Sharma, T. Goel, M. Tanveer, P. N. Suganthan, I. Razzak and R. Murugan, "Conv-eRVFL: Convolutional Neural Network Based Ensemble RVFL Classifier for Alzheimer's Disease Diagnosis," in IEEE Journal of Biomedical and Health Informatics, vol. 27, no. 10, pp. 4995-5003, Oct. 2023, doi: 10.1109/JBHI.2022.3215533.

[15] B. Guelib, K. Zarour, H. Hermessi, B. Rayene and K. Nawres, "Same-Subject-Modalities-Interactions: A Novel Framework for MRI and PET Multi-Modality Fusion for Alzheimer's Disease Classification," in IEEE Access, vol. 11, pp. 48715-48738, 2023, doi: 10.1109/ACCESS.2023.3276722.

[16] X. Gao, H. Cai and M. Liu, "A Hybrid Multi-Scale Attention Convolution and Aging Transformer Network for Alzheimer's Disease Diagnosis," in IEEE Journal of Biomedical and Health Informatics, vol. 27, no. 7, pp. 3292-3301, July 2023, doi: 10.1109/JBHI.2023.3270937.

[17] F. Mercaldo, M. D. Giammarco, F. Ravelli, F. Martinelli, A. Santone and M. Cesarelli, "TriAD: A Deep Ensemble Network for Alzheimer Classification and Localization," in IEEE Access, vol. 11, pp. 91969-91980, 2023, doi: 10.1109/ACCESS.2023.3307702.

[18] X. Gao, H. Liu, F. Shi, D. Shen and M. Liu, "Brain Status Transferring Generative Adversarial Network for Decoding Individualized Atrophy in Alzheimer's Disease," in IEEE Journal of Biomedical and Health Informatics, vol. 27, no. 10, pp. 4961-4970, Oct. 2023, doi: 10.1109/JBHI.2023.3304388.

[19] R. Sharma, T. Goel, M. Tanveer, C. T. Lin and R. Murugan, "Deep-Learning-Based Diagnosis and Prognosis of Alzheimer's Disease: A Comprehensive Review," in IEEE Transactions on Cognitive and Developmental Systems, vol. 15, no. 3, pp. 1123-1138, Sept. 2023, doi: 10.1109/TCDS.2023.3254209.

[20] K. Oh, J. S. Yoon and H. -I. Suk, "Learn-Explain-Reinforce: Counterfactual Reasoning and its Guidance to Reinforce an Alzheimer's Disease Diagnosis Model," in IEEE Transactions on Pattern Analysis and Machine Intelligence, vol. 45, no. 4, pp. 4843-4857, 1 April 2023, doi: 10.1109/TPAMI.2022.3197845.

[21] L. Yu, J. Liu, Q. Wu, J. Wang and A. Qu, "A Siamese-Transport Domain Adaptation Framework for 3D MRI Classification of Gliomas and Alzheimer's Diseases," in IEEE Journal of Biomedical and Health Informatics, vol. 28, no. 1, pp. 391-402, Jan. 2024, doi: 10.1109/JBHI.2023.3332419.

[22] C. Li et al., "Individualized Assessment of Brain Aβ Deposition With fMRI Using Deep Learning," in IEEE Journal of Biomedical and Health Informatics, vol. 27, no. 11, pp. 5430-5438, Nov. 2023, doi: 10.1109/JBHI.2023.3306460.

[23] H. Cai, Y. Gao and M. Liu, "Graph Transformer Geometric Learning of Brain Networks Using Multimodal MR Images for Brain Age Estimation," in IEEE Transactions on Medical Imaging, vol. 42, no. 2, pp. 456-466, Feb. 2023, doi: 10.1109/TMI.2022.3222093.

[24] C. Bass et al., "ICAM-Reg: Interpretable Classification and Regression With Feature Attribution for Mapping Neurological Phenotypes in Individual Scans," in IEEE Transactions on Medical Imaging, vol. 42, no. 4, pp. 959-970, April 2023, doi: 10.1109/TMI.2022.3221890.

[25] H. Zhang et al., "Classification of Brain Disorders in rs-fMRI via Local-to-Global Graph Neural Networks," in IEEE Transactions on Medical Imaging, vol. 42, no. 2, pp. 444-455, Feb. 2023, doi: 10.1109/TMI.2022.3219260.